

A Powder Neutron Diffraction Study of Semiconducting and Metallic Niobium Dioxide

Adrian A. Bolzan, Celesta Fong, and Brendan J. Kennedy¹

Department of Inorganic Chemistry, The University of Sydney, Sydney NSW 2006, Australia

and

Christopher J. Howard

*Australian Nuclear Science and Technology Organization, Lucas Heights Research Laboratories,
Private Mail Bag 1, Menai NSW 2234, Australia*

Received September 20, 1993; in revised form December 28, 1993; accepted January 3, 1994

Rietveld analysis of neutron powder diffraction patterns from niobium dioxide at 295 and 1300 K have been performed. At 1300 K NbO₂ adopts a rutile-type structure ($P4_2/mnm$, $a = 4.8463 \text{ \AA}$, $c = 3.0315 \text{ \AA}$, $x = 0.2924$), whereas the room temperature form can be described as a superstructure with a subcell of the rutile type ($I4_1/a$, $a = 13.7020 \text{ \AA}$, $c = 5.9850 \text{ \AA}$). Both the c axis and the oxygen position parameter in the rutile phase are anomalously small compared with other rutile dioxides. This can be rationalized in terms of $M-M$ bonding. Both the niobium and the oxygen thermal displacement are large in the rutile phase. © 1994 Academic Press, Inc.

INTRODUCTION

Niobium dioxide, like a select number of other metal oxides, undergoes a metal-insulator transformation accompanied by a crystallographic phase transition (1, 2). Compared with the numerous studies on the transition in the isoelectronic VO₂ system (3, 4) there is a scarcity of information on NbO₂ (5-9). This is partially a result of the higher transition temperature of NbO₂, 800°C (5), relative to VO₂, in which the transition occurs at 70°C (3).

X-ray diffraction studies have shown that both VO₂ (3) and NbO₂ (4) adopt a regular rutile structure in their high-temperature forms, while the low-temperature structures are usually described as "distorted rutiles." The rutile structure is one of the simplest MO₂ structures, tetragonal space group $P4_2/mnm$ (No. 136), with M at (000) and O at ($xx0$). Hence the structure is fully described by three parameters, namely, the cell parameters a and c and the oxygen position parameter x . In the case of VO₂ the low-temperature phase is monoclinic (10) (C_{2h}^5 ($P2_1/c$), with

four formula units per cell), while NbO₂ is a more complex body-centered tetragonal structure (8) (C_{4h}^6 ($I4_1/a$), with 32 formula units per cell). Despite this the two room temperature structures have a number of common features, the most distinctive being the alternately longer and shorter $M-M$ distances running in the c -axis direction.

Whereas the structure of the rutile phase of VO₂ has been accurately determined by a single-crystal X-ray study (3), similar accurate studies of the rutile phase of NbO₂ do not appear to have been reported. A comparison of the structures of transition metal oxides which adopt the rutile structure indicates that both the oxygen position parameter and the thermal displacements in the rutile phase of VO₂ are unusual (3-11). The large thermal parameters in VO₂ are indicative of lattice softening, and similarly large thermal parameters should be present in rutile NbO₂. Goodenough has described a phenomenological model to explain the basic structural properties of the common metal dioxides. Over the past 10 years there have been a number of attempts to explain the precise structural properties of this class of compounds (12-15). In one of the more comprehensive studies Burdett (12) has suggested that oxide lattice energetics are important in stabilizing the two phases, and in particular the small oxygen position parameter in VO₂, $x = 0.3000$, (3) compared to $x = 0.306$ in TiO₂ (16) may be related to the stability of the distorted structure. A similarly small oxygen position parameter might therefore be predicted to occur in NbO₂. The available powder X-ray measurements have clearly demonstrated the structure of NbO₂ above the transition temperature, but they have not provided a determination of either the oxygen position or the thermal displacements of the atoms.

High-resolution powder neutron diffraction studies are, in principle, capable of accurately determining both the

¹ To whom correspondence should be addressed.

TABLE 1
Details of Data Collection and Refinement

	Temperature (°C)	
	25	1000
Neutron wavelength (Å)	1.500	1.372
2 θ scan range (°)	20–160	20–160
2 θ scan step size (°)	0.05	0.05
Maximum step intensity	10 ⁴	2 × 10 ⁴
No. of reflections	662	58
No. of refined parameters	36	18
R_{wp} (%)	5.64	4.23
R_{exp} (%)	4.26	3.41
R_B (%)	1.36	4.29

oxygen position parameter and thermal vibrations in the rutile NbO₂. As compared with VO₂, NbO₂ is more amenable to study by neutron diffraction. Despite the relative stability of the Nb(IV) oxidation state, at high temperatures it is rapidly oxidized by atmosphere to Nb₂O₅ or it can be further reduced to NbO (17). Thus any structural study needs to be performed under carefully controlled conditions, both of atmosphere and of temperature. In powder neutron diffractometry it is relatively easy to study materials at high temperatures. In the present work we have studied the structures of both phases of NbO₂ using powder neutron diffraction.

EXPERIMENTAL

A polycrystalline sample of NbO₂ was prepared by reduction of Nb₂O₅ (Aldrich) under flowing hydrogen at 950°C for 48 hr. Powder X-ray diffraction data confirmed the presence of single-phase highly crystalline NbO₂. X-ray photoelectron spectroscopy failed to detect any metal impurities.

Powder neutron diffraction patterns were recorded on the high-resolution powder diffractometer (HRPD) at the Australian Nuclear Science and Technology Organisation's HIFAR reactor (18). Room temperature measurements were made with the sample contained in a thin-walled vanadium can. For high-temperature measurements the sample was contained in an evacuated silica ampoule. Other details are given in Table 1. Rietveld method (19) structural analysis was carried out using the program LHPM1 (20).

RESULTS

The space group, $I4_1/a$, and starting values for the least-squares refinement of the low-temperature structure of NbO₂ were taken from Cheetham and Rao (21). There are six independent atoms in the unit cell, two Nb and four

O. The atoms were constrained to vibrate isotropically, and initially it was assumed that the thermal vibrations of the two Nb were equal, as were the vibrations of the four O atoms. An insignificant improvement in the fit was obtained when this constraint was removed, R_{Bragg} decreasing from 1.37 to 1.36%, and as seen from Table 2 the thermal parameters for the four independent O atoms and for the two independent Nb atoms are essentially the same. This is in agreement with Pynn *et al.* (8) who found that while the thermal vibrations are anisotropic in NbO₂, the parameters for the independent oxygens and niobiums each have approximately the same values. Figure 1 shows the fit between the observed and the calculated diffraction patterns. The structural parameters are given in Table 2, and the measures of fit are in Table 1. Derived interatomic distances are recorded in Table 3. The final values of the lattice parameters $a = 13.7020(2)$ and $c = 5.9850(1)$ Å and the atomic positions are in good agreement with both the powder neutron diffraction study by Cheetham and Rao (21) and the single-crystal neutron study by Pynn *et al.* (8).

The diffraction pattern collected at 1000°C shows only lines due to a rutile-type structure, there being no lines indicative of a superstructure. It is immediately apparent from the decreasing intensities with increasing angle observed in the high-temperature diffraction pattern that the thermal motions of the atoms are considerably larger than those at room temperature. Refinement of the high-temperature structure was commenced using the lattice parameters reported by Sakata *et al.* (6), an oxygen position parameter, $x = 0.3000$, and isotropic thermal parameters. The silica ampoule resulted in an undulating background, and as a consequence of this the background was not refined, but rather estimated by interpolation between 30 points. Early in the refinement it became apparent that while the literature a and c parameters were reasonable, the oxygen parameter had an unusually low value, $x = 0.2924$. In the final stage of the refinement anisotropic thermal parameters were included. The nonrefinement of the background results in an apparently high R_{Bragg} value

TABLE 2
Atomic Coordinates and Thermal Parameters for the Room Temperature Structure of NbO₂

	x	y	z	B_{iso} (Å ²)
Nb(1)	0.1150(2)	0.1254(4)	0.4766(3)	0.26(3)
Nb(2)	0.1349(2)	0.1247(4)	0.0271(3)	0.33(4)
O(1)	0.9863(3)	0.1285(6)	-0.0038(14)	0.52(7)
O(2)	0.9758(3)	0.1303(5)	0.4999(15)	0.46(7)
O(3)	0.2746(3)	0.1261(6)	0.9995(15)	0.49(6)
O(4)	0.2641(3)	0.1231(6)	0.5044(14)	0.60(6)

Note. The value in parentheses is the estimated standard deviation in the last place.

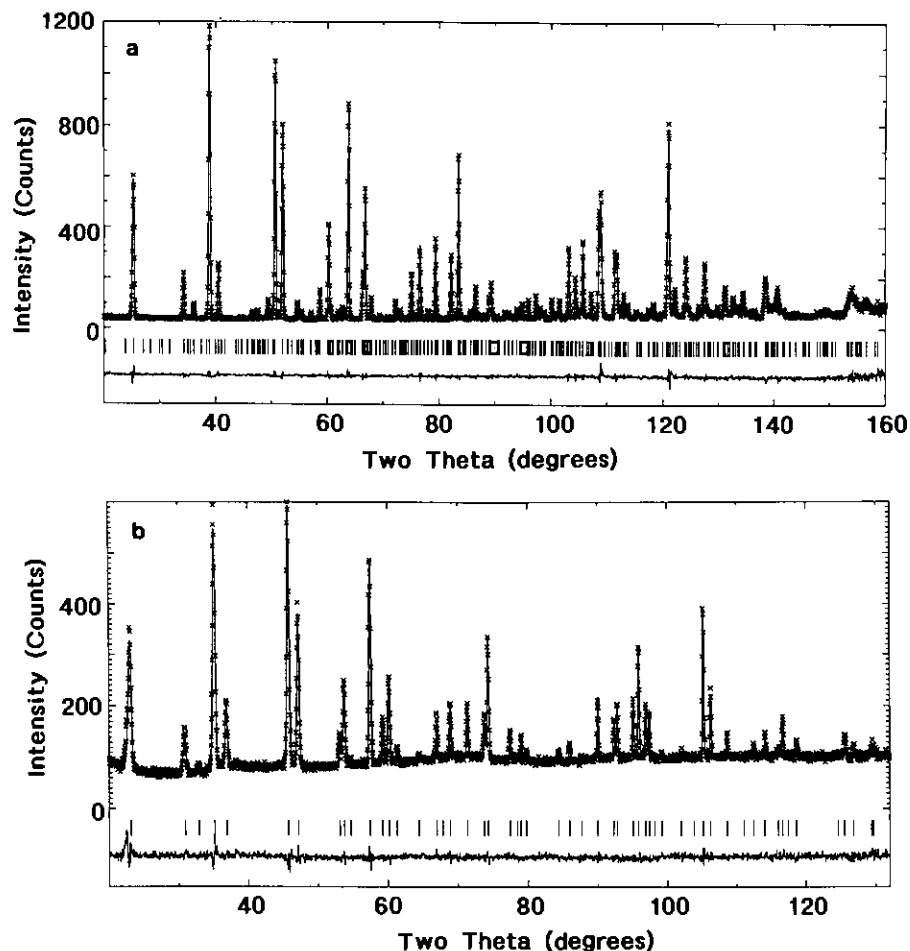


FIG. 1. Neutron powder patterns of NbO_2 (a) at room temperature and (b) at 1000°C . The difference between the observed data (\times) and the calculated profile (solid line) is shown in the lower trace. All allowed reflections are marked by vertical lines.

(22); however, as evident from Fig. 1 the agreement between the observed and the calculated diffraction profiles is excellent. The structural parameters and measures of fit are given in Tables 4 and 1, respectively.

TABLE 3
Selected Interatomic Distances (\AA) in the Room Temperature Structure of NbO_2

Bond	Distance	Bond	Distance
Nb(1)–Nb(2)	2.71	Nb(2')–O(22)	2.06
Nb(1)–Nb(2')	3.30	Nb(2')–O(32)	2.25
Nb(1)–O(2)	1.91	Nb(2')–O(11)	2.05
Nb(1)–O(41)	1.92	Nb(2')–O(13)	1.95
Nb(1)–O(22)	2.25	Nb(2)–O(12)	1.95
Nb(1)–O(4)	2.05	Nb(2)–O(31)	1.92
Nb(1)–O(32)	2.05	Nb(2)–O(41)	2.14
Nb(1)–O(12)	2.13	Nb(2)–O(1)	2.05
Nb(2')–O(3)	1.92	Nb(2)–O(33)	2.25
Nb(2')–O(42)	2.14	Nb(2)–O(21)	2.09

DISCUSSION

The current determination of the structure of the low-temperature phase of NbO_2 is in excellent agreement with the previous single-crystal neutron diffraction study (8). The low-temperature structure consists of NbO_6 octahedra which are joined by edges and corners as in the ideal rutile structure. The Nb–Nb distances along the edge-sharing chains, that is, along the c axis, are alternately 2.71 and 3.30 \AA , corresponding to pairing of the metal atoms (Fig. 2). This metal atom pairing is very likely the result of Peierls instability (2, 7). The NbO_6 form distorted octahedra, with Nb–O bond lengths between 1.91 and 2.25 \AA . The displacement of the Nb atoms from the octahedral centers results in a buckling of the octahedra and an alternation of the oxygen atoms (Fig. 2).

The high-temperature form of NbO_2 adopts a four long + two short Nb–O bond pattern. This is opposite to that seen in a number of other rutile structures including TiO_2 (16) and VO_2 (3); however, it is by no means a rare occurrence (11, 21). The c/a ratio is low, 0.6255,

TABLE 4
Atomic Coordinates and Thermal
Parameters for NbO₂ at 1000°C

Lattice parameters (Å)	
<i>a</i>	4.8463(1)
<i>c</i>	3.0315(1)
<i>x</i> position parameter	0.2924(2)
Thermal parameters (Å ² × 10 ³)	
Nb <i>U</i> ₁₁ ^a	22.1(5)
<i>U</i> ₁₂	0.8(6)
<i>U</i> ₁₁ + <i>U</i> ₁₂	23(1)
<i>U</i> ₁₁ - <i>U</i> ₁₂	21(1)
<i>U</i> ₃₃	34(1)
O <i>U</i> ₁₁	30.9(6)
<i>U</i> ₁₂	-9.7(5)
<i>U</i> ₁₁ + <i>U</i> ₁₂	21(1)
<i>U</i> ₁₁ - <i>U</i> ₁₂	41(1)
<i>U</i> ₃₃	26.6(8)
Bond distances (Å)	
×4 Nb-O	2.079(3)
×2 Nb-O	2.005(1)
Nb-Nb ^b	3.0315(1)
Nb-Nb ^c	3.747(8)
O··O ^d	2.844(2)

Note. The value in parentheses is the estimated standard deviation in the last place.

^a See text for explanation of these parameters.

^b The Nb-Nb distance along [001] is the *c* parameter.

^c Shortest Nb-Nb distance along [111].

^d Shortest O-O distance across the shared edge.

compared with typical values of 0.6441 in TiO₂ (16) or 0.6917 for the only other rutile-type dioxide with a partially filled 4*d* shell, RuO₂ (11). The *c/a* value is comparable with that found in the rutile phase of VO₂, 0.6250 (3), where the *a* value appears normal, but the *c* value is small. McWhan *et al.* (3) noted the small *c* value in VO₂ and related this to the short V-V distance across the edge. At first glance the observed *c* value in the high-temperature phase of NbO₂ does not appear to be unusual, 3.0315 Å, compared with 2.9587 Å in TiO₂; however, note that as the ionic radius of the metal increases the unit cell dimensions are expected to increase (11). It is therefore inappropriate to compare the main structural parameters of NbO₂ with the 3*d* analogues such as TiO₂ or MnO₂, but rather they should be compared with 4*d* compounds where the ionic radii of the metal are similar. In doing this the *c* value in NbO₂ is seen to be noticeably shorter than that found in, for example, RuO₂ (24, 25). It might be possible that the low *c/a* value in the rutile NbO₂ phase is a conse-

quence of anisotropic thermal expansion in the structure as the temperature increases. The superstructure of the low-temperature NbO₂ structure can, however, be related to a pseudo-rutile cell by $a = 2\sqrt{2} * a_r$ and $c = 2c_r$, where a_r and c_r correspond to the parameters of the pseudo-rutile cell (29). It is found that the *c/a* ratio at room temperature is smaller than that at 1000°C. In fact *a* is found to be essentially invariant to temperature, increasing marginally from 4.844 Å at 25°C to 4.846 Å at 1000°C, where *c* increases by 0.039 Å from 2.993 to 3.032 Å over the same temperature range. The small *c* value in NbO₂ is not a result of anisotropic thermal expansion, but rather indicates the presence of Nb-Nb bonding.

In VO₂ it is unclear if the onset of metallic conductivity results from direct overlap of the V 3*d* orbitals across the closest contact in the rutile structure or if overlap involves the bridging oxygen atoms. The larger ionic radii of Nb(IV), 0.74 Å, compared to V(IV), 0.63 Å, suggest that direct overlap of the partially filled 4*d* orbitals will be more important in NbO₂. In NbO₂ it appears likely that the very short Nb-Nb distance, 3.0315 Å, results from the formation of a Nb-Nb bond. A second unusual feature in the high-temperature structure is the anomalously low value of the oxygen position parameter, $x = 0.2924$. This is the lowest value found in any of the regular rutile compounds (23, 24). Rutile-type VO₂ also has a low value of x , 0.3000, which, as McWhan *et al.* (3) noted, results in only a slight distortion of the VO₆ octahedra. Both the oxygen position parameter x and the lattice parameters are related to the Nb-O bond lengths in the rutile structure,

$$d_a = \sqrt{2} * xa$$

$$d_e = \{2(1/2 - x)^2 a^2 + (c/2)^2\}^{1/2}.$$

The two variables, x and *c/a*, have opposite effects; as the value of *c/a* decreases the equatorial *M*-O distance d_e decreases, whereas a decrease in x results in an increase in d_e but a decrease in the axial bond length d_a . In the present case the small value of x reflects the need of the lattice to avoid close contact between the oxygen atoms at the shared edges of the octahedra (distance = $\sqrt{a} - 2\sqrt{2} * xa$), thus reducing electrostatic repulsion. For *c/a* = 0.6255, the closest O-O distance increases from 2.7415 Å at $x = 0.3000$ to the observed value of 2.8443 Å at $x = 0.2925$. These distances are not absolutely short; in stishovite (rutile-type SiO₂) the O-O distance across the shared edge is very short, 2.29 Å (27).

Burdett has shown that for a fixed *M*-O bond length the regular rutile structure is favored over the distorted variant by smaller x values (12). This observation neglects the role of the *M*-*M* interactions along the *c* axis, which are of course independent of x , in stabilizing the regular structure. As noted by Burdett (12) and more recently by

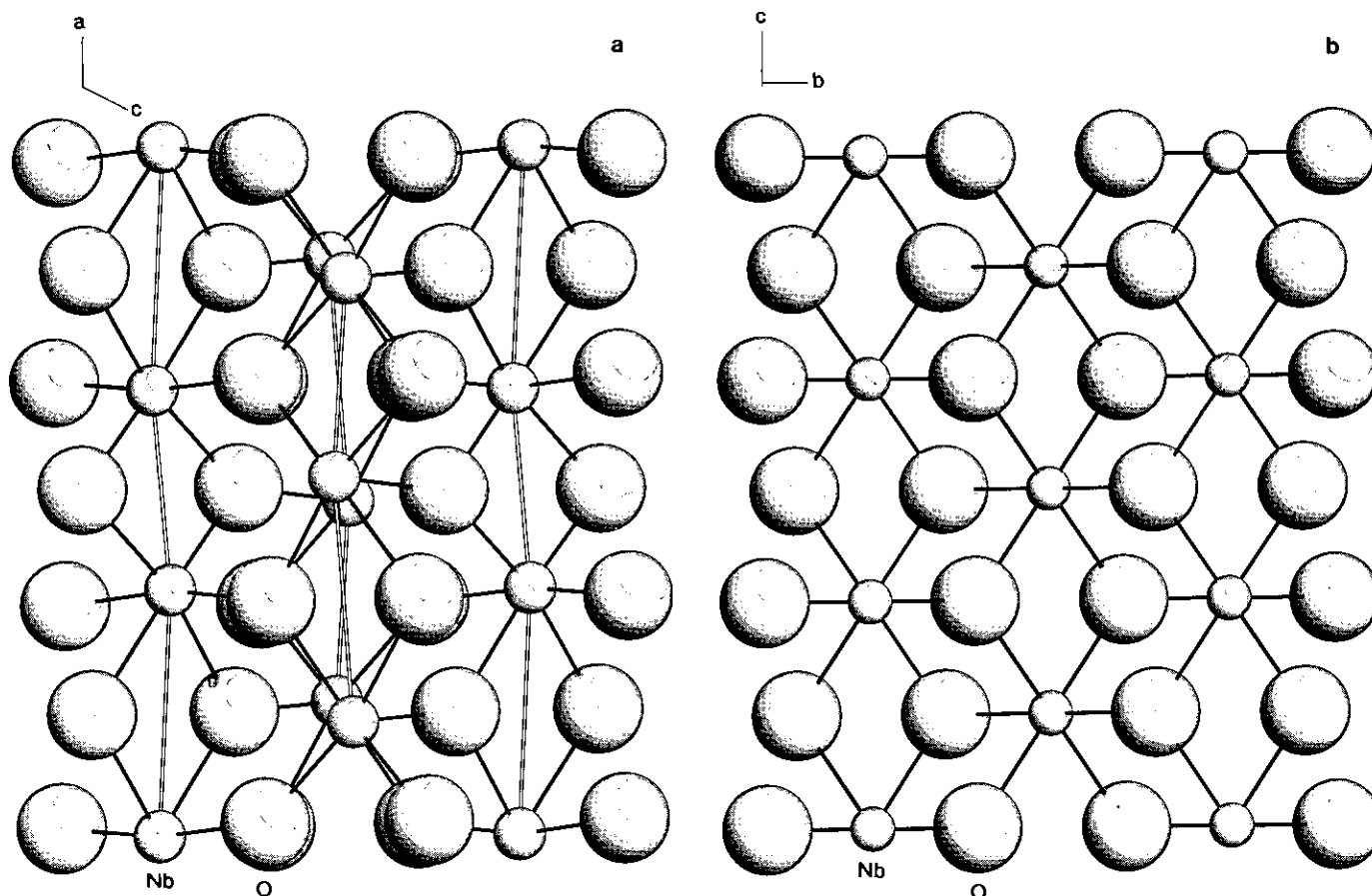


FIG. 2. Comparison of (a) room temperature and (b) high-temperature structures of NbO_2 . The displacement of the Nb atoms from the octahedral centers in the room temperature structure results in a puckering of the octahedra.

Sorantin and Schwarz (15), the ground-state geometry of a metal dioxide is determined by the interplay between a number of factors including O-O and M - M interactions. Undoubtedly if the c/a ratio is small, as occurs in NbO_2 , then it is necessary for the oxygen to be displaced away from the "normal" position of $x = 0.305$. Currently available models do not appear to be capable of accurately calculating the exact extent of this displacement (14, 15).

Finally, it is appropriate to comment on the large thermal vibrations observed in the rutile-type NbO_2 structure. As indicated above in VO_2 , large, anisotropic, thermal displacements in the rutile phase have been interpreted as evidence for lattice softening. In the case of NbO_2 it is less clear how appropriate this explanation is, since although a single soft mode frequency has been identified, no low-frequency phonon branches have been detected. The anisotropic nature of the O vibrations is easily rationalized since the stereochemistry in the rutile structure is such that the "in-plane" thermal displacements of the oxygen atoms are strongly favored. The thermal vibrations in NbO_2 are obviously considerably larger than those found in TiO_2 at 1060°C (28); however, they show similar

anisotropy, with the dominant mean squared vibrational amplitude being $U_{11}-U_{12}$, which occurs in the (001) planes, perpendicular to the linear O-Nb-O moieties. This thermal vibration is characteristic of the rutile-type structure and has been observed in a number of other dioxides with the rutile structure (11, 16, 24, 29). As originally noted by McWhan (3) for VO_2 and seen in the present study of NbO_2 , the oxygen vibrations are unusually large in these two rutiles. It is apparent that the precise determination of the structures of both regular and distorted rutiles is likely to enhance our understanding of both thermal vibrations and of the relationship between c/a and the oxygen position parameter.

ACKNOWLEDGMENT

We thank the Australian Institute for Nuclear Science and Engineering for partial support for this research.

REFERENCES

1. J. B. Goodenough, *Prog. Solid State Chem.* **5**, 145 (1971).
2. N. F. Mott, "Metal-Insulator Transitions." Taylor and Francis, London, 1974.

3. D. B. McWhan, M. Marezio, J. P. Remeika, and P. D. Dernier, *Phys. Rev. B* **10**, 490 (1974).
4. W. Paul, *Mater. Res. Bull.* **5**, 691 (1970).
5. G. Belanger, J. Destry, G. Perluzzo, and P. M. Raccach, *Can. J. Phys.* **52**, 2272 (1974).
6. T. Sakata, K. Sakata, and I. Nishida, *Phys. Status Solidi* **27**, 1183 (1986).
7. S. M. Shapiro, J. D. Axe, G. Shirane, and P. M. Raccach, *Solid State Commun.* **15**, 377 (1974).
8. R. Pynn, J. D. Axe, and R. Thomas, *Phys. Rev. B* **13**, 2965 (1976).
9. R. Pynn, J. D. Axe, and P. M. Raccach, *Phys. Rev. B* **17**, 2196 (1978).
10. J. M. Longo and P. Kierkegaard, *Acta Chem. Scand.* **24**, 420 (1970).
11. C. Fong, Thesis, The University of Sydney, 1991.
12. J. K. Burdett, *Inorg. Chem.* **24**, 2244 (1985).
13. J. K. Burdett, T. Hughbanks, G. J. Miller, J. W. Richardson, and J. V. Smith, *J. Am. Chem. Soc.* **109**, 3639 (1987).
14. J. K. Burdett, G. J. Miller, J. W. Richardson, and J. V. Smith, *J. Am. Chem. Soc.* **110**, 8064 (1988).
15. P. I. Sorantin and K. Schwarz, *Inorg. Chem.* **31**, 567 (1992).
16. C. J. Howard, T. M. Sabine, and F. Dickson, *Acta Crystallogr. Sect. B* **47**, 462 (1991).
17. F. A. Cotton and G. Wilkinson, "Advanced Inorganic Chemistry," 5th ed. Interscience, New York, 1988.
18. C. J. Howard, C. J. Ball, R. L. Davis, and M. M. Elcombe, *Aust. J. Phys.* **36**, 507 (1983).
19. H. M. Rietveld, *J. Appl. Crystallogr.* **2**, 65 (1969).
20. R. J. Hill and C. J. Howard, Australian Atomic Energy Commission Report No. M112, 1986.
21. A. K. Cheetham and C. N. R. Rao, *Acta Crystallogr. Sect. B* **32**, 1579 (1976).
22. R. J. Hill and R. X. Fischer, *J. Appl. Crystallogr.* **23**, 462 (1990).
23. W. H. Baur, *Acta Crystallogr. Sect. B* **32**, 2200 (1976).
24. C. Fong, B. J. Kennedy, A. A. Bolzan, and C. J. Howard, submitted for publication.
25. K. V. Krishna and L. Iyengar, *Acta Crystallogr. Sect. A* **25**, 302 (1969).
26. B. O. Marinder, *Acta. Chem. Scand.* **15**, 707 (1961).
27. R. J. Hill, M. D. Newton, and G. V. Gibbs, *J. Solid State Chem.* **47**, 185 (1983).
28. K. Sugiyama and Y. Takeuchi, *Z. Kristallogr.* **307** (1991).
29. A. A. Bolzan, C. Fong, B. J. Kennedy, and C. J. Howard, *Aust. J. Chem.* **46**, 939 (1993).